InternationalJournalofEngineeringInnovationsinAdvancedTechnology
ISSN:2582-1431(Online),Volume-5 Issue-1,March 2023

Image Background Detection And Enhancement Of Colour Image Using Morphological Contrast

Srikanth Veesam, N. SalmaSulthana
Assistant Professor, Dept of ECE, Princeton Institute of Engineering and Technology for Women, Hyderabad, TS, India,
E-mail: veesamsrikanth@gmail.com.
Assistant Professor, Dept of ECE, Princeton Institute of Engineering and Technology for Women, Hyderabad, TS, India,
E-mail: salmasulthana4u@gmail.com.

***Abstract*— In this paper, some morphological transformations are used to detect the background in images characterized by poor lighting. Lately, contrast image enhancement has been carried out by the application of two operators based on the Weber's law notion. The first operator employs information from block analysis, while the second transformation utilizes the opening by reconstruction, which is employed to define the multibackground notion. The objective of contrast operators consists in normalizing the grey level of the input image with the purpose of avoiding abrupt changes in intensity among the different regions. Finally, the performance of the proposed operators is illustrated through the processing of images with different backgrounds, the majority of them with poor lighting conditions.**

***Index Terms*—Image background, morphological contrast, morphological filters by reconstruction, multibackground, Weber's law.**

I. INTRODUCTION

THE contrast enhancement problem in digital images can be approached from various methodologies, among which is mathematical morphology (MM). Initial studies on contrast enhancement in this area were carried out by Meyer and Serra [1], who introduced the contrast mappings notion. Such operators consist in accordance to some proximity criterion, in selecting for each point of the analyzed image, a new grey level between two patterns (primitives) [1]. Other works based on the contrast mapping concept have been developed elsewhere [2]–[4]. With regard to MM, several studies based on contrast multiscale criterion have been carried out [5]–[7]. In the work proposed by Mukhopadhyay and Chanda [6], a scheme is de- fined to enhance local contrast based on a morphological top-hat transformation. While Kasperek [7] implements a processing system in real time for its application in the enhancement of angiocardiographic images, based on the work carried out by Mukhopadhyay.

Manuscript received Mar 1, 2031; Revised Mar 26, 2023; Accepted March 30, 2023

Even though morphological contrast has been largely studied, there are no methodologies, from the point of view MM, capable of simultaneously normalizing and enhancing the contrast in images with poor lighting. On the other side, one of the most common techniques in image processing to enhance dark regions is the use of nonlinear functions, such as logarithm or power functions [8]; otherwise, a method that works in the frequency domain is the homomorphic filter [9]. In addition, there are techniques based on data statistical analysis, such as global and local histogram equalization. During the histogram equalization process, grey level intensities are reordered within the image to obtain an uniform distributed histogram [10]. How- ever, the main disadvantage of histogram equalization is that the global properties of the image cannot be properly applied in a local context [11], frequently producing a poor performance in detail preservation. In [12], a method to enhance contrast is proposed; the methodology consists in solving an optimization problem that maximizes the average local contrast of an image. The optimization formulation includes a perceptual constraint derived directly from human suprathreshold contrast sensitivity function. In [12], the authors apply the proposed operators to some images with poor lighting with good results. On the other hand, in [13], a methodology to enhance contrast based on color statistics from a training set of images which look visually ap- pealing is presented. Here, the basic idea is to select a set of training images which look good perceptually, next a Gaussian mixture model for the color distribution in the face region is built, and for any given input image, a color tone mapping is performed so that the color statistics in the face region matches the training examples. In this way, even though the reported algorithms to compensate changes in lighting are varied, some are more adequate than others.

In this work, two methodologies to compute the image background are proposed. Also, some operators to enhance and normalize the contrast in grey level images with poor lighting are introduced. Contrast operators are based on the logarithm function in a similar way to Weber's law [8], [14]. The use of the logarithm function avoids abrupt changes in lighting. Also, twoapproximations to compute the background in the processed images are proposed. The first proposal consists in an anal- ysis by blocks, whereas in the second proposal, the opening by reconstruction is used given its following properties: a) it passes through regional minima, and b) it merges components of the image without considerably modifying other structures.

Finally, this paper is organized as follows. Section II presents a brief background on Weber's law and some morphological transformations. Section III gives an approximation to the background by means of block analysis in conjunction with transformations that enhance images with poor lighting. In Section IV, the multibackground notion is introduced by means of the opening by reconstruction. Section V shows a comparison among several techniques to improve contrast in images. Finally, conclusions are presented in Section VI.

I. Morphological Transformations and Weber's Law

A background on morphological transformations is presented below.

A. Definitions of Some Morphological Transformations

In mathematical morphology, increasing and idempotent transformations are frequently used. Morphological transformations complying with these properties are known as morphological filters [17]–[19]. The basic morphological filters are the morphological opening $\gamma_{\mu B}(f)(x)$ and closing $\varphi_{\mu B}(f)(x)$ using a given structural element. In this paper, a square structuring element is employed, where B represents the structuring element of size 3 3 pixels, which contains its origin. While $\check{B}$ is the transposed set $(\check{B} = \{-x : x \in B\})$ and μ is a homothetic parameter. Formally, the morphological opening $\gamma_{\mu B}(f)(x)$ and closing $\varphi_{\mu B}(f)(x)$ are expressed as follows:

$$\begin{aligned} &\gamma_{\mu B}(f)(x) = \delta_{\mu\check{B}}\left(\varepsilon_{\mu B}(f)\right)(x) \\ \text{And}\quad &\varphi_{\mu B}(f)(x) = \varepsilon_{\mu\check{B}}\left(\delta_{\mu B}(f)\right)(x) \end{aligned} \tag{1}$$

Where the morphological erosion $\varepsilon_{\mu B}(f)(x)$ and the morphological dilation $\delta_{\mu B}(f)(x)$ are $\varepsilon_{\mu B}(f)(x) = \wedge\{f(y) : y \in \mu\check{B}_x\}$ and $\delta_{\mu B}(f)(x) = \vee\{f(y) : y \in \mu\check{B}_x\}$, respectively. Here, $\wedge$ is the inf operator and $\vee$ is the sup operator.

On the other hand, throughout the paper, we will use either size 1 or size μ for the structuring element. Size 1 means a square of 3 3 pixels, while size μ means a square of $(2\mu+1)(2\mu+1)$ pixels. For example, if the structuring element is size 3, then the square will be 7×7 pixels, to render an analysis of 49 neighboring regions. For any size of the structuring element, the origin is located at its center.

B. Opening and Closing by Reconstruction

The reconstruction transformation notion is a useful concept introduced by MM. These transformations allow the elimination of undesirable regions without considerably affecting the remaining structures of the image. This characteristic arises from the way in which these transformations are built by means of geodesic transformations [20]. The geodesic dilation $\delta_f^1(g)(x)$ and the geodesic erosion $\varepsilon_f^1(g)(x)$ of size one are given by $\delta_f^1(g)(x) = f(x) \wedge \delta(g)(x)$ with $g(x) \leq f(x)$ and $\varepsilon_f^1(g)(x) = f(x) \vee \varepsilon(g)(x)$ with $g(x) \geq f(x)$, respectively. When the function $g(x)$ is equal to the erosion (dilation, respectively) of the original function, we obtain the opening

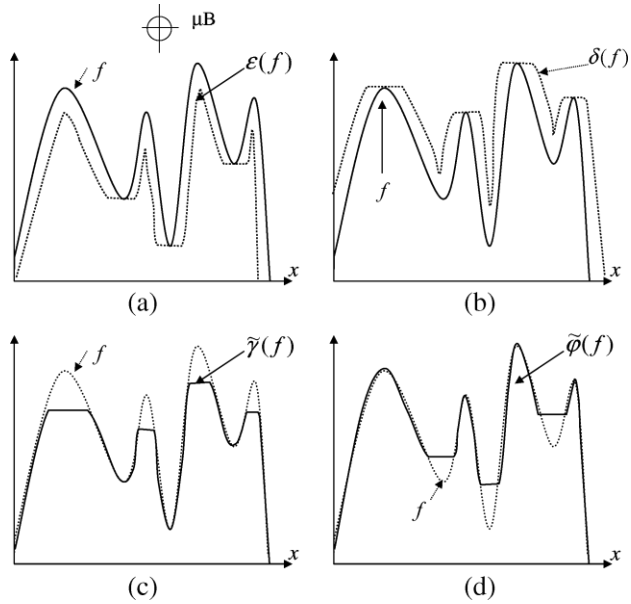

Fig. 1. (a) Original image and marker , (b) original image and marker , (c) opening by reconstruction using erosion as marker, (d) Closing by reconstruction using dilation as marker.

$\tilde{\gamma}_{\mu B}(f)(x)$ (Closing $\tilde{\varphi}_{\mu B}(f)(x)$ respectively) by reconstruction, i.e., [15], [16], [21]

$$\begin{aligned} \tilde{\gamma}_{\mu B}(f)(x) &= \lim_{n\to\infty} \delta_f^n\left(\varepsilon_{\mu B}(f)\right)(x) \\ \text{and}\quad \tilde{\varphi}_{\mu B}(f)(x) &= \lim_{n\to\infty} \varepsilon_f^n\left(\delta_{\mu B}(f)\right)(x). \end{aligned} \tag{2}$$

In Fig. 1, the performance of the opening and closing by reconstruction is illustrated. Note in Fig. 1(c) and 1(d) that some components have been eliminated, while the remaining are maintained equal to the original image. In this paper, regional maxima or minima are defined as follows [21].

Definition 1: A regional maximum M (regional minimum m, respectively) of a grayscale image f is a connected component of pixels with a given value h (plateau of altitude h), such that every pixel in the neighborhood of M (m respectively) has a strictly lower(upper, respectively) value.

C. Weber's Law

In psycho-visual studies, the contrast C of an object with luminance $L_{\max}$ against its surrounding luminance $L_{\min}$ is de- fined as follows [22]:

$$C = \frac{L_{\max} - L_{\min}}{L_{\min}}. \tag{3}$$

If $L = L_{\min}$ and $\triangle L = L_{\max} - L_{\min}$, (3) can be rewritten as

$$C = \frac{\triangle L}{L}. \tag{4}$$

Equation (4) indicates that $\triangle(logL)$ is proportional to C; therefore, Weber's law can be expressed as [8]

$$C = klogL + b \qquad L > 0 \tag{5}$$

where k and b are constants, b being the background.

ISSN:2582-1431(Online),Volume-5 Issue-1,March 2023

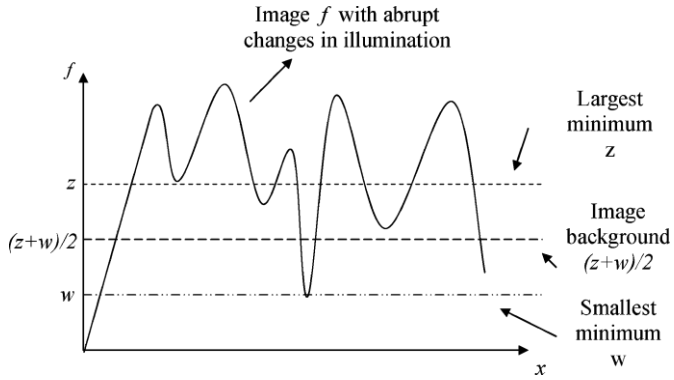

Fig. 2. Background detection from the smallest and largest minima of the image.

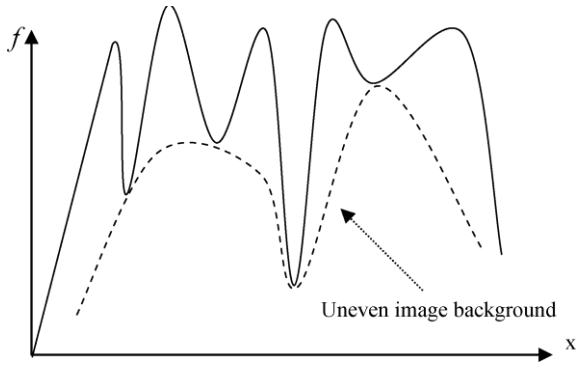

Fig. 3. Uneven background (dashed line) in images with poor lighting.

In our case, an approximation to Weber's law is considered by taking the luminance L as the grey level intensity of a function f (image); in this way, expression (5) is written as

$$C = klog\, f + b \qquad f > 0. \tag{6}$$

On the other hand, in [23], a methodology to compute the background parameter [b in (5)] was proposed. The methodology consists in calculating the average between the smallest and largest regional minima, as illustrated in Fig. 2. However, the main disadvantage of this proposal is that the image background is not detected in a local way. As a result, the contrast is not correctly enhanced in images with poor lighting, since considerable changes occur in the image background due to abrupt changes in luminance as illustrated in Fig. 3.

In the next section, a proposal to compute the image background by blocks is introduced.

II. Image Background Approximation by Blocks

In this paper, D represents the digital space under study, with $D = Z^2$ and Z the integer set. In this way, let D be the domain of definition of the function f. The image f is divided into n blocks w^i of size $l_1 \times l_2$. Each block is a subimage of the original image. The minimum and maximum intensity values in each subimage are denoted as

$$m_i = \wedge\, w^i(x) \qquad \forall x \in D_{w^i} \subseteq D \tag{7}$$

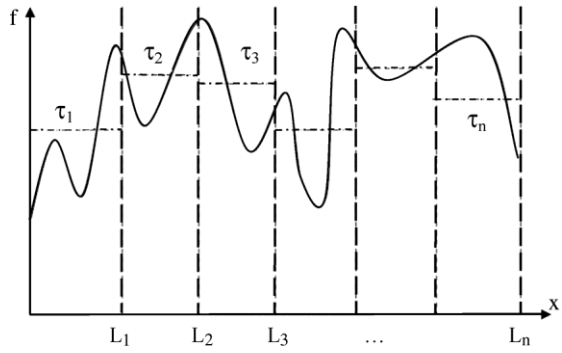

Fig. 4. Background criteria obtained by block analysis.

$$M_i = \vee\, w^i(x) \qquad \forall x \in D_{w^i} \subseteq D. \tag{8}$$

For each analyzed block, maximum (M_i) and minimum (m_i) values are used to determine the background criteria τ_i in the following way:

$$\tau_i = \frac{m_i + M_i}{2} \qquad \forall i = 1, 2, \ldots, n. \tag{9}$$

In the 1-D case, as illustrated in Fig. 4, the following expression is obtained:

$$\nu(x) = \begin{cases} \tau_1 & x \le L_1 \\ \tau_2 & L_1 < x \le L_2 \\ \tau_3 & L_2 < x \le L_3 \\ & \cdot \\ \tau_n & L_{n-1} < x \le L_n. \end{cases}$$

The value of τ_i represents a division line between clear $(f > \tau_i)$ and dark $(f \le \tau_i)$ intensity levels. Once τ_i is calculated, this value is used to select the background parameter associated with the analyzed block. As follows, an expression to enhance the contrast is proposed:

$$\Gamma_{\tau_i}(f) = \begin{cases} k_i log(f+1) + M_i, & f \le \tau_i \\ k_i log(f+1) + m_i, & \text{otherwise.} \end{cases} \tag{10}$$

Note that the background parameter depends on the τ_i value. If $f \le \tau_i$ (dark region), the background parameter takes the value of the maximum intensity (M_i) within the analyzed block, and the minimum intensity (m_i) value otherwise. Also, the unit was added to the logarithm function in (10) to avoid indetermination. On the other hand, since grey level images are used in this paper, the constant k_i in (10) is obtained as follows:

$$k_i = \frac{255 - m_i^*}{\log(256)} \qquad \forall i = 1, 2, \ldots, n$$

with

$$m_i^* = \begin{cases} m_i, & f > \tau_i \\ M_i, & f \le \tau_i. \end{cases}$$

Equation (10) works similar to a contrast mapping [1], which modifies the intensity values depending on certain criterion. The criterion to modify the contrast in (10) is given by τ_i. On the

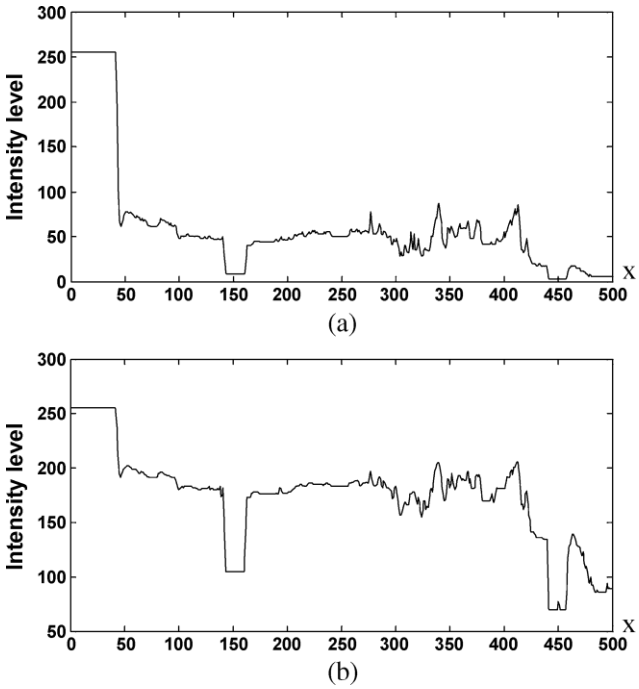

Fig. 5. Performance of equation (10) in a 1-D signal. (a) Original signal; (b) output signal after applying equation (10).

other hand, M_i and m_i values are used as background parameters to improve the contrast depending on the τ_i value, due to the background is different for clear and dark regions. An example to illustrate the performance of (10) considering a 1-D signal is presented in Fig. 5. Notice that, in this figure, the intensity levels are stretched in an important way due to: i) the behavior of the logarithm function; and ii) the background parameter M_i or m_i.

In this way, the transformation $\Gamma_{\tau_i}(f)$ fulfills the next properties.

Property 1: **a)** *It is a nonincreasing transformation*, i.e., for any two images f_1 and f_2 with $f_1 \leq f_2$, $\Gamma_{\tau_i}(f_1) \geq \Gamma_{\tau_i}(f_2)$; **b)** *it is not an idempotent transformation, that is,* $\Gamma_{\tau_i}\Gamma_{\tau_i}(f) \neq \Gamma_{\tau_i}(f)$; **c)** *it is an extensive transformation, i.e.,* $f \leq \Gamma_{\tau_i}(f)$; **d)** *it is possible to classify the definition domain of* f *in two sets*: the set S_{τ_i} composed by high contrast areas, (for every point $x \in S_{\tau_i}$, $f > \tau_i$) and the set $S^c_{\tau_i}$ composed by low contrast areas (for every point $x \in S^c_{\tau_i}$, $f \leq \tau_i$); **e)** the composition of contrast mappings using (10) will result in lighter images for each iteration, reaching a limit imposed by the value of the highest level of intensity of the image, $\text{maxint} = 255$ in our particular case, that is, $\underbrace{\Gamma_{\tau_i} \ldots \Gamma_{\tau_i}(\Gamma_{\tau_i}(f))}_{n \text{ times}} \rightarrow \text{maxint}$; and **f)** if image f is subdivided into smaller blocks each time, the background function $b(x)$ tends to be similar to the original function f. □

On the other hand, given that, maximum and minimum values are analyzed for each block, an extension using morphological operators is presented as follows.

Let $I_{\max}(x)$ and $I_{\min}(x)$ be the the maximum and minimum intensity values taken from one set of pixels contained in a window (B) of elemental size (3×3 elements), $x \in D$. Notice that the window corresponds to the structuring element B. For the sake of simplicity, let us consider $I_{\max}(x) = \max\{f(x+b) : b \subseteq B\}$ and $I_{\min}(x) = \min\{f(x+b) : b \subseteq B\}$, $x \in D$. Then, from (9), a new expression is derived

$$\tau(x) = \frac{I_{\min}(x) + I_{\max}(x)}{2} \tag{11}$$

where $I_{\max}(x)$ and $I_{\min}(x)$ values correspond to the morphological dilation and erosion defined by the order-statistical filters [24]. Thus, (11) is expressed as

$$\tau(x) = \frac{\varepsilon_\mu(f)(x) + \delta_\mu(f)(x)}{2}. \tag{12}$$

Notice that τ_i was substituted by $\tau(x)$, since $\tau(x)$ has a local character given by the structuring element μB. In this way, the contrast operator in (10) is written as

$$\Gamma_{\tau(x)}(f) = \begin{cases} k_{\tau(x)} log(f+1) + \delta_\mu(f)(x), & f \leq \tau(x) \\ k_{\tau(x)} log(f+1) + \varepsilon_\mu(f)(x), & \text{otherwise} \end{cases}$$
$$\text{and} \quad k_{\tau(x)} = \frac{255 - \tau(x)}{\log(256)}. \tag{13}$$

To illustrate the performance of (10) and (13), some output images are presented.

Application example for (10): Consider the input image in Fig. 6(a1). The τ values for each block in Fig. 6(a2) are: $\tau_1 = 10, \tau_2 = 1, \tau_3 = 2$ and $\tau_4 = 1$. The enhanced image is presented in Fig. 6(a3). Other examples are presented in Fig. 6(a4)–(a7). Original images are given in Fig. 6(a4) and (a6), while Fig. 6(a5) and (a7) are the enhanced images. On the other hand, image in Fig. 6(b1) was taken from a database developed by Belhumeur and Georghiades [25]. The image in Fig. 6(b2) illustrates the background image considering 20 blocks, while the improved image is presented in Fig. 6(b3). Notice that, in the enhanced images, abrupt changes in illumination are avoided. In addition, objects not visible in the original images are revealed.

Application example for (13): A better local analysis is achieved when (13) is applied instead of (10) to detect the background criterion $\tau(x)$. This situation occurs, because the structuring element μB allows the analysis of sets of neighboring pixels at each point in the image. If size μ increases, more pixels will be taken into account to compute such parameter. Fig. 7 illustrates the performance of (13). Original images are located in Fig. 7(a) and (b) while enhanced images are presented in Fig. 7(c) and (d). These improved images were obtained with $\mu = 1$. Notice that several characteristics not visible at first sight appear in the enhanced images.

III. Image Background Determination Using the Opening by Reconstruction

It is desirable to obtain a function that resembles the image background without dividing the original image into blocks, and without using the morphological erosion and dilation, since these morphological transformations generate new contours when the structuring element is increased. This situation is illustrated in Fig. 8. When morphological erosion or dilation

ISSN:2582-1431(Online),Volume-5 Issue-1,March 2023

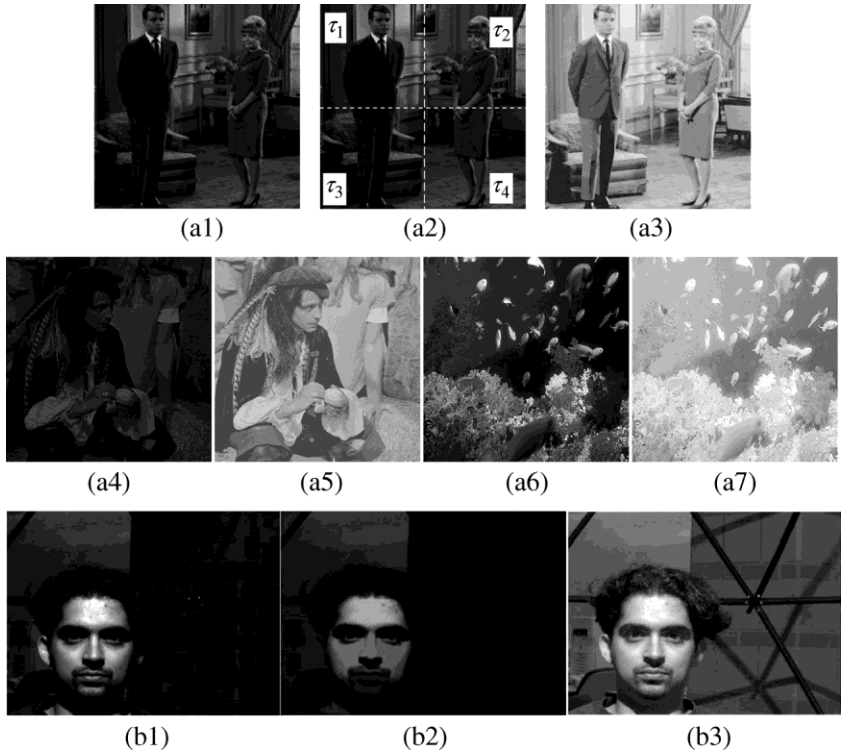

Fig. 6. Image background detection using block approach and contrast enhancement. (a1) Original image, (a2) image divided into four blocks. The values of for each block are $_1$; $_2$; $_3$ and $_4$; (a3) enhanced image after applying equation (10); (a4), (a6) original images; (a5), (a7) enhanced images after applying equation (10); (b1) original image; (b2) image background considering 20 blocks; and (b3) enhanced image after applying equation (10).

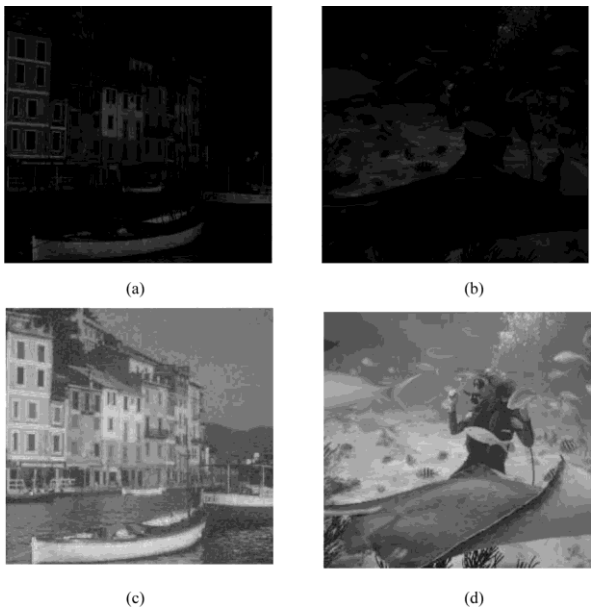

Fig. 7. Image background detection using the morphological erosion and dilation. (a), (b) Original images; (c), (d) enhanced images after applying equation (13).

are used with large sizes of to reveal the background, inappropriate values may be obtained. However, in MM, there is other class of transformations that allows the filtering of the image without generating new components; these transformations are called transformations by reconstruction (see Section II-B). In our case, the opening by reconstruction is our choice because touches the regional minima and merges regional maxima [21]. This characteristic allows the modification of the altitude of regional maxima when the size of the structuring element increases. This effect can be used to detect the background criteria $(\tau(x))$ in (9), i.e.,

$$\tau(x) = \tilde{\gamma}_{\mu}(f)(x). \tag{14}$$

Equation (10) is maintained and only the way to detect the background is modified. An example of this modification is shown in Fig. 9. Input images are located in Fig. 9(a) and (c), whereas enhanced images are presented in Fig. 9(b) and (d). The image background criteria [$\tau(x)$ in (14)] was calculated with a structuring element size 10 for all output images.

On the other hand, it is possible to use the opening by reconstruction to generate the image background similarly to that presented in Fig. 3, and not only, as a criterion to detect the background as was presented in (14).

An uneven background (dashed line) is illustrated in Fig. 3, which is detected from an image with important variations in lighting. Observe that the background touches only regional minima, while the other regions contain local information of the original function. From these extreme points and the local information provided by the original function (in other words the background), important information about the image can be acquired.

When considering the opening by reconstruction to detect the background, one further operation is necessary to detect

ISSN:2582-1431(Online),Volume-5 Issue-1,March 2023

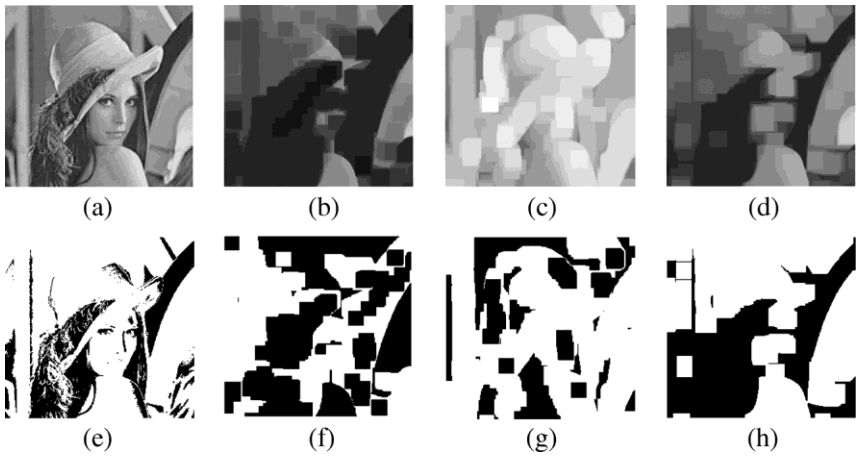

Fig. 8. Output images illustrating the generation of new contours. (a) Original image, (b) erosion size , (c) dilation size , (d) Opening size , (e), (f), (g), (h) Threshold of the images in (a), (b), (c), and (d).

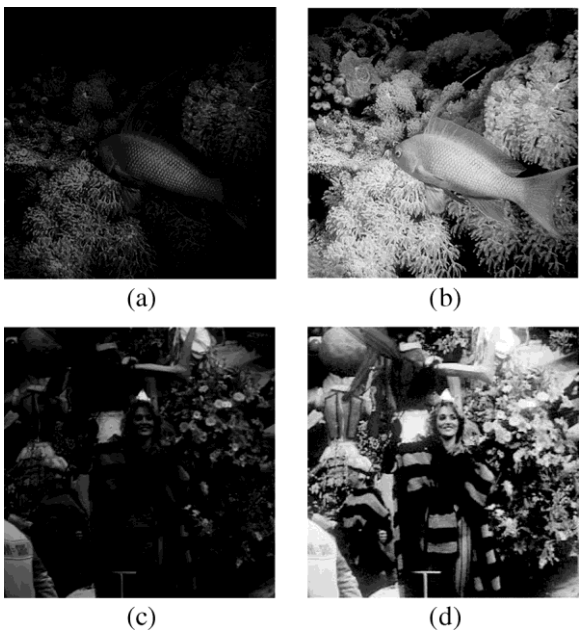

Fig. 9. Opening by reconstruction as background criteria. (a), (c) Original images; (b), (d) enhanced images considering the opening by reconstruction as background criterion.

the local information given by the original function (image extremes are contained in the opening by reconstruction because of its behavior). The morphological transformation proposed for this task is the erosion size $\mu = 1$, i.e. [see (6)]

$$b(x) = \varepsilon_1 [\tilde{\gamma}_\mu(f)](x). \tag{15}$$

This idea is illustrated in Fig. 10. Given that the morphological erosion tends to generate new information when the structuring element is enlarged, in this study, the image background was computed by using only the morphological erosion size 1.

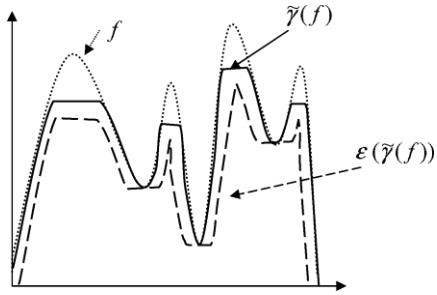

Fig. 10. Image background obtained from the erosion of the opening by reconstruction.

Thus, the following expression derived from (6) is proposed to enhance the contrast in images with poor lighting

$$\xi_{\tilde{\gamma}_\mu}(f) = k(x)log(f+1) + \varepsilon_1[\tilde{\gamma}_\mu(f)]$$

$$\text{and} \qquad = \frac{\text{maxint} - \varepsilon_1[\tilde{\gamma}_\mu(f)]}{\text{Log}(\text{maxint}+1)}. \tag{16}$$

In our case, the maximum grey level is $\text{maxint} = 255$. If the background image increases, the image tends to become lighter due to the additive effect of the image background. Formally, we have

$$\lim_{\varepsilon_1[\tilde{\gamma}_\mu(f)](x)\to\text{maxint}} \xi_{\tilde{\gamma}_\mu}(f) = \text{maxint}. \tag{17}$$

Considering that the morphological erosion size $\mu = 1$ is fixed in (16), properties a), b), c), and d) mentioned in Properties 1 are also fulfilled by operator $\xi_{\tilde{\gamma}_\mu}(f)$. However, an interesting property is obtained from the behavior of the opening by reconstruction. This property is called *multibackground* and is presented as follows.

Property 2 (Multibackground): For all $\mu_1 > 0$, $\mu_2 > 0$, and $\mu_1 < \mu_2$ such that $\tilde{\gamma}_{\mu_1}(f) \geq \tilde{\gamma}_{\mu_2}(f)$, then $\varepsilon_1[\tilde{\gamma}_{\mu_1}(f)](x) \geq \varepsilon_1[\tilde{\gamma}_{\mu_2}(f)](x)$.

The multibackground property allows the generation of a family of image backgrounds when the size of the structuring element μ is increased. This situation is illustrated in Fig. 11, where (15) is applied. The original image is presented in Fig. 11(a). A

ISSN:2582-1431(Online),Volume-5 Issue-1,March 2023

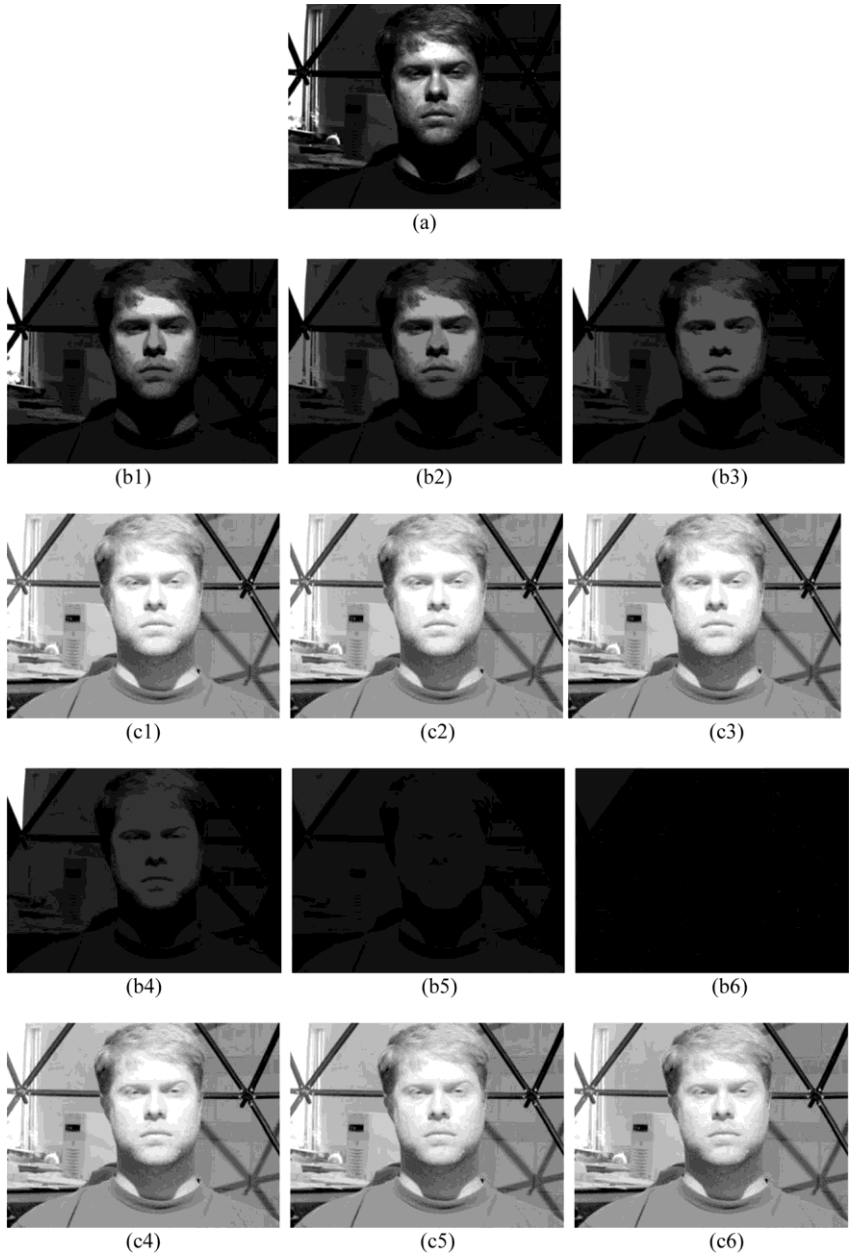

Fig. 11. Image background using the opening by reconstruction with different sizes. (a) Original image; (b1), (b2), (b3), (b4), (b5), (b6) background images obtained after applying equation (15) with structuring element sizes 10, 20, 30, 40, 50, and 60; (c1), (c2), (c3), (c4), (c5), (c6) enhanced images obtained from the application of equation (16).

set of output background images is presented in Fig. 11(b1)–(b6). These output images are obtained from (15) with $\mu = 10$, 20, 30, 40, 50, and 60, respectively, while the enhanced images, obtained after applying (16), are shown in Fig. 11(c1)–(c6).

Other example is presented in Fig. 12. Original images are shown in Fig. 12(a)–(c) and (g), whereas enhanced images obtained from (16) can be observed in Fig. 12(d)–(f) and (h).

The histograms of some images obtained from the picture located in Fig. 13(a1) are presented in Fig. 13. The purpose of Fig. 13 is to illustrate the changes produced in the enhanced image when the background is modified by the application of (16). The background of the image was detected for $\mu = 10$, 20, and 30. The histograms of the processed images [see Fig. 13(a2)–(a4)] can be observed in Fig. 13(b2)–(b4). Notice that, for each size μ, different histograms are obtained.

IV. Comparison With Other Contrast Operators

Two methodologies to enhance the contrast have been proposed in [12] and [13]. In Fig. 14, a comparison between output image obtained from (16) and the output image provided in the paper by Liu *et al.* [13] was carried out. These authors propose to modify the contrast by means of a data base of images with good contrast; the contrast is enhanced basically by considering the information located in the face following a learning procedure. The original image is located in Fig. 14(a), whereas the output images obtained with the methodology given in [13] and our proposal are presented in Fig. 14(b) and (c), respectively. The image in Fig. 14(c) [obtained with (16)] presents an over- illumination effect in some regions; this situation occurs because the original image does not was captured in poor lighting conditions,

ISSN:2582-1431(Online),Volume-5 Issue-1,March 2023

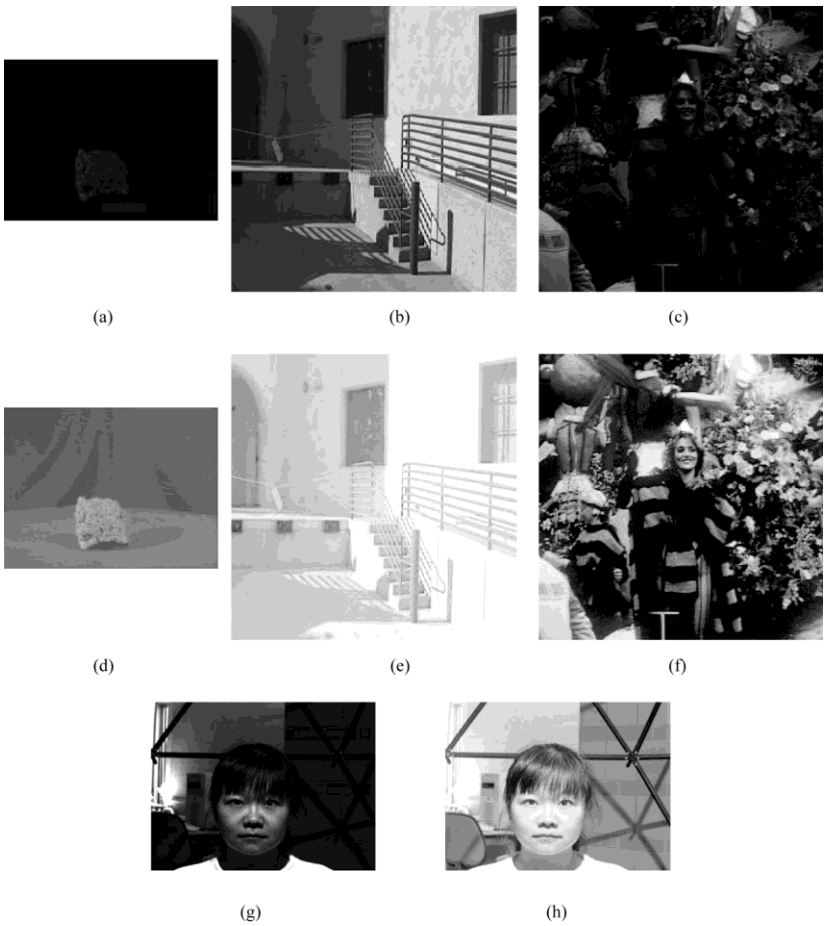

Fig. 12. Image background obtained from the opening by reconstruction. (a), (b), (c), (g) Original images; (d), (e), (f), (h) enhanced images after applying equation (16).

due to this, the logarithm function produces an over-illuminating effect when applied to the processed image. Due to this situation, contrast enhancement in Fig. 14(b) is better that in Fig. 14(c).

On the other hand, in Fig. 15, the performance of (16) is compared with other transformations provided in the literature. The original image is presented in Fig. 15(a), whereas the image in Fig. 15(b) is obtained from the equalization histogram. This technique is widely used to improve images with poor lighting. As mentioned in the introduction, the histogram equalization technique consists in reordering the grey level intensities within the image to obtain an uniformly distributed histogram [10].

The output image in Fig. 15(c) was obtained from a morphological transformation introduced by Meyer and Serra [1]; the following contrast mapping was applied:

$$W_\mu f(x) = \begin{cases} a_1\varphi_\mu(f)(x), & 0 \le \rho(x) < \beta \\ f(x), & \beta \le \rho(x) < \alpha \\ a_2\gamma_\mu(f)(x), & \alpha \le \rho(x) \le 1 \end{cases} \quad (18)$$

$$\rho(x) = \frac{\varphi_\mu(f)(x) - f(x)}{\varphi_\mu(f)(x) - \gamma_\mu(f)(x)} \quad (19)$$

where a_1 and a_2 are constants, with $a_1 = a_2 = 2$, the opening and closing size is $\mu = 3$, while parameters α and β are equal to 0.125. On the other hand, the output image in Fig. 15(d) was obtained by applying the methodology provided by Majumder and Irani [12] with $\tau = 2$ (parameter τ employed in [12] has a different meaning to that in our work). Finally, Fig. 15(e) was obtained by applying (16) (transformation proposed in this work).

In analyzing Fig. 15, notice in the image located in Fig. 15(b) the presence of over-illuminated regions on the face. In Fig. 15(c), several regions have been degraded, while other areas are over-illuminated. The output image in Fig. 15(d) was obtained with the methodology proposed in [12] with $\tau = 2$, this image was hardly enhanced, and remain many regions with poor lighting. Finally, the output image in Fig. 15(e) was obtained with (16). Notice in Fig. 15(e) that not only abrupt transitions of illumination are avoided [which do not occur in Fig. 15(b), (c), and (d)], but also several face characteristics are revealed. On the other hand, unlike techniques as histogram equalization and morphological contrast mappings, among others, the methodologies introduced in this paper are appropriate for images whose main feature is a deficient illumination. In the case of applying the proposed operators to images with correct lighting, over-illuminated images will be obtained (see Fig. 16). This effect is due to the logarithm function, which normalizes grey level intensities by dismissing changes in illumination. In a future work, this problem will be treated.

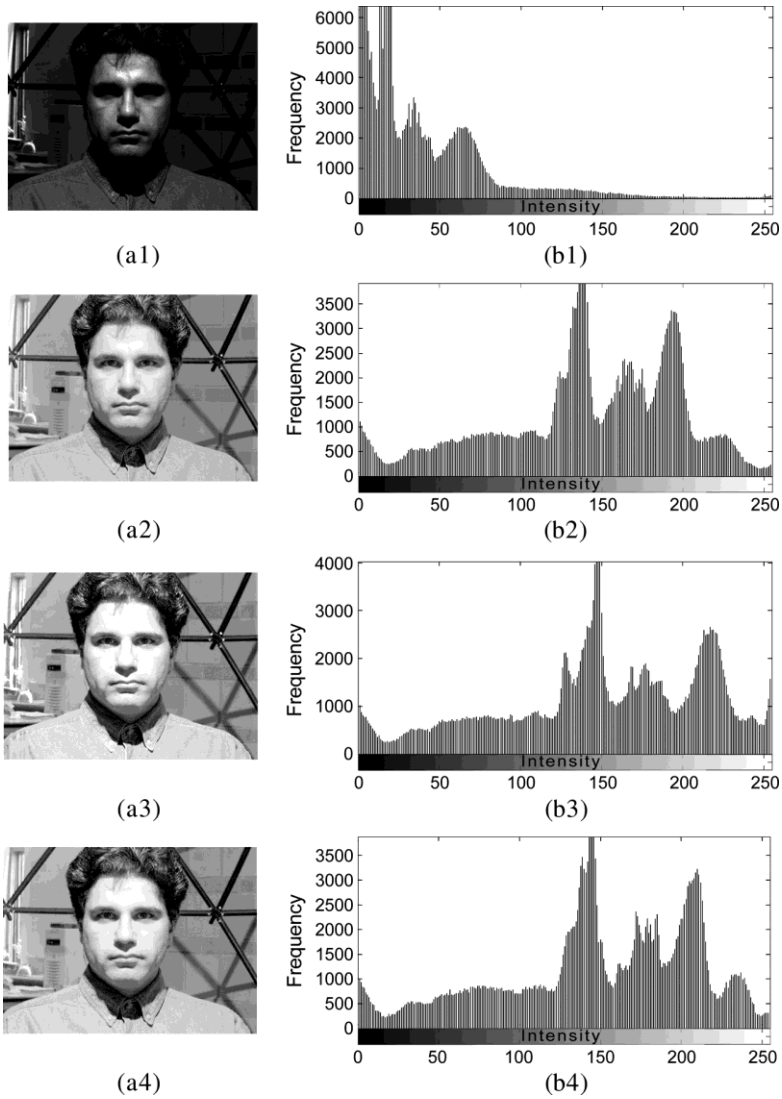

Fig. 13. (a1) Original image; (b1) histogram of the image in Fig. 13(a1); (a2), (a3), (a4) Enhanced images using $_1$ $_\mu$ as background with 10, 20, and 30; (b2), (b3), (b4) corresponding histograms of the images in Figs. 13(a2), (a3), (a4).

VI. Conclusion

This paper presents a study to detect the image background and to enhance the contrast in grey level images with poor lighting. First, a methodology was introduced to compute an approximation to the background using blocks analysis. This proposal was subsequently extended using mathematical morphology operators. However, a difficulty was detected when the morphological erosion and dilation were employed; therefore, a new proposal to detect the image background was propounded, that is based on the use of morphological connected transformations.

Also, morphological contrast enhancement transformations were introduced. Such operators are based on Weber's law notion. These contrast transformations are characterized by the normalization of grey level intensities, avoiding abrupt changes inillumination. Theperformanceofthepropos alsprovidedinthis work were illustrated by means of several examples throughout thepaper. Also, theoperatorsperformanceemployedinthispaper werecomparedwithothersgivenintheliterature. Finally, adisadvantage of contrast enhancement transformations studied in this paper is that they can only be used satisfactorily in images with poor lighting; in a future work this problem will be considered.

Appendix A

Properties fulfilled by the morphological dilation $\delta_\mu(f)(x)$, erosion $\varepsilon_\mu(f)(x)$, and opening by reconstruction $\tilde{\gamma}_\mu(x)$ [18], [19], [21].

1) $\delta_\mu(f)(x)$ is an extensive transformation, i.e., $f(x) \leq \delta(f)(x)$.
2) $\varepsilon_\mu(f)(x)$ is an antiextensive transformation, i.e., $f(x) \geq \varepsilon(f)(x)$.
3) $\delta_\mu(f)(x)$ *and* $\varepsilon_\mu(f)(x)$ *are increasing transformations*, that is, given $f(x)$ and $g(x)$ with $g(x) \leq f(x)$, then $\varepsilon(g)(x) \leq \varepsilon(f)(x)$ and $\delta(g)(x) \leq \delta(f)(x)$.
4) Property of the opening by reconstruction $\tilde{\gamma}_\mu(f)(x)$.

Given $\mu_1 > 0$, $\mu_2 > 0$, with $\mu_1 < \mu_2$, then

$$\tilde{\gamma}_{\mu_1}(f) \geq \tilde{\gamma}_{\mu_2}(f). \tag{20}$$

Properties of the Operator in (10):

1) *It is a nonincreasing transformation*. Let $f(x)$ and $g(x)$ be two functions, with $g(x) \leq f(x)$. We suppose that the

ISSN:2582-1431(Online),Volume-5 Issue-1,March 2023

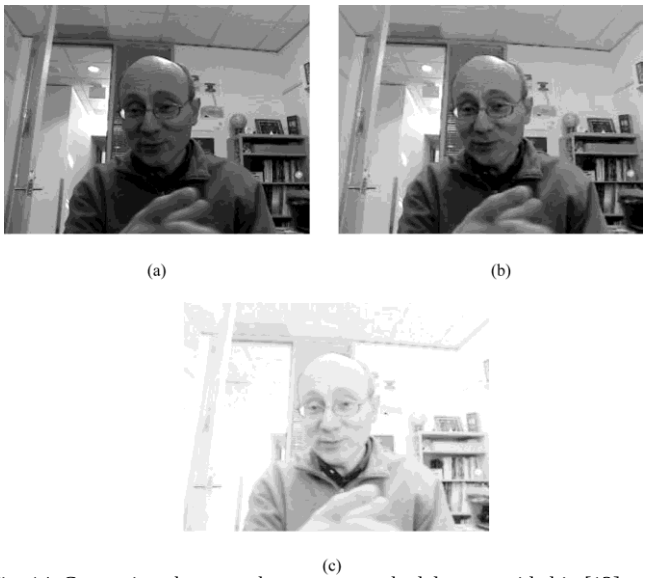

Fig. 14. Comparison between the contrast methodology provided in [13] and our work. (a) Original image, (b) enhanced image obtained from the methodology introduced in [13], and (c) output image obtained from the application of equation (16) (proposal introduced in this work).

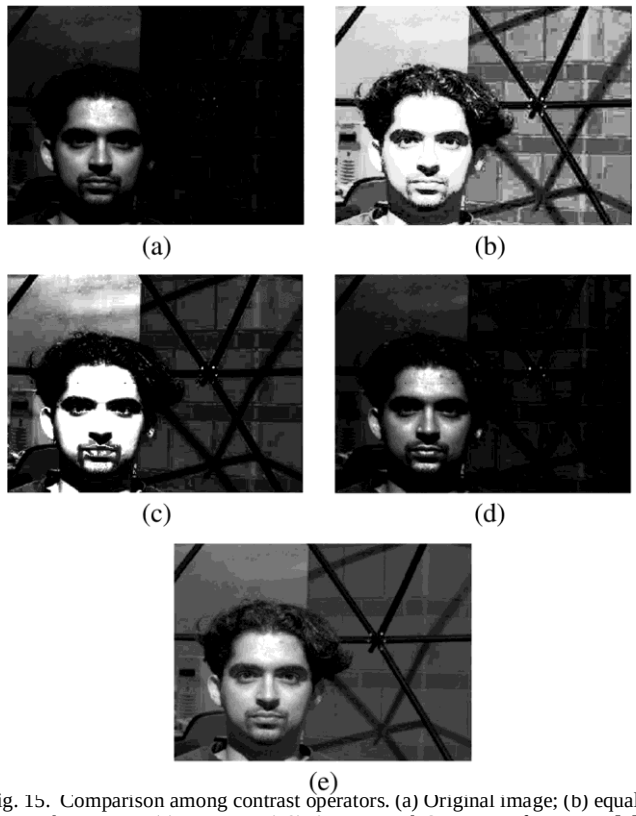

Fig. 15. Comparison among contrast operators. (a) Original image; (b) equalization histogram; (c) equation (18) (Meyer and Serra transformation [1]); (d) output image obtained from the proposal given by Majumder and Irani [12]; and (e) equation (16) (proposal introduced in this work).

number of blocks n is given and finite, and let i be the i^{th} block. Then

$$m_i(g) \leq m_i(f)$$
$$M_i(g) \leq M_i(f) \tag{21}$$

so

$$\tau_i(g) = \frac{m_i(g) + M_i(g)}{2} \leq \frac{m_i(f) + M_i(f)}{2} = \tau_i(f). \tag{22}$$

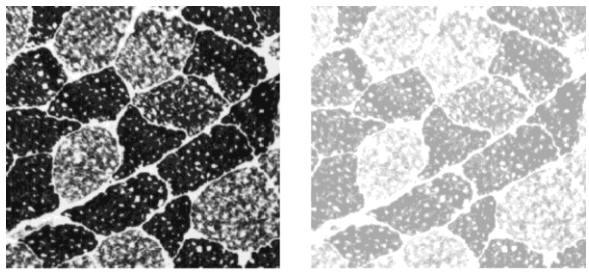

Fig. 16. Normal lighting. (a) Image with normal lighting, and (b) enhanced image obtained from the application of equation (16) (proposal introduced in this work).

On the other hand

$$m_i^*(g) \leq m_i^*(f)$$
$$-m_i^*(g) \geq -m_i^*(f)$$
$$255 - m_i^*(g) \geq 255 - m_i^*(f)$$

Consequently

$$k_i(g) = \frac{255 - m_i^*(g)}{\log(256)} \geq \frac{255 - m_i^*(f)}{\log(256)} = k_i(f). \tag{23}$$

Also, since $g \leq f$, then

$$g + 1 \leq f + 1$$
$$\log(g+1) \leq \log(f+1)$$

However, the increasing property for (23) is not satisfied.

2) *It is not an idempotent transformation*. In fact

$$\Gamma_{\tau_i}(\Gamma_{\tau_i}(f)) \neq \Gamma_{\tau_i}(f).$$

3) *It is an extensive transformation*. In fact

$$f(x) \leq \Gamma_{\tau_i}(f)(x).$$

Property of the Operator in (16): > 0 And

1) ***Multibackground***. For all $\mu_1 > 0$, μ_2 , $\geq$ $\mu_1 < \mu_2, \Rightarrow \tilde{\gamma}_{\mu_1}(f) \geq \tilde{\gamma}_{\mu_2}(f)$, then $\varepsilon_1[\tilde{\gamma}_{\mu_1}(f)](x)$ $\varepsilon_1[\tilde{\gamma}_{\mu_2}(f)](x)$. This property may be intuitively derived From (20).

ACKNOWLEDGMENT

The authors would like to thank Dr. A. Majumder and Dr. Z. Liu for the images provided to complete this work.

REFERENCES

[1] F. Meyer and J. Serra, "Contrast and Activity Lattice," *Signal Process.*, vol. 16, pp. 303–317, 1989.
[2] I. R. Terol-Villalobos, "Morphological image enhancement and segmentation," in *Advances in Imaging and Electron Physics*, P. W. Hawkes, Ed. New York: Academic, 2001, pp. 207–273.
[3] I. R. Terol-Villalobos, "Morphological connected contrast mappings based on top-hat criteria: A multiscale contrast approach," *Opt. Eng.*, vol. 43, no. 7, pp. 1577–1595, 2004.
[4] J. D. Mendiola-Santibañez and I. R. Terol-Villalobos, "Morphological contrast mappings based on the flat zone notion," *Computación y Sistemas*, vol. 6, pp. 25–37, 2002.
[5] A. Toet, "Multiscale contrast enhancement with applications to image fusion," *Opt. Eng.*, vol. 31, no. 5, 1992.
[6] S. Mukhopadhyay and B. Chanda, "A multiscale morphological approach to local contrast enhancement," *Signal Process.*, vol. 80, no. 4, pp. 685–696, 2000.
[7] J. Kasperek, "Real time morphological image contrast enhancement in virtex FPGA," in *Lecture Notes in Computer Science*. New York: Springer, 2004.

ISSN:2582-1431(Online),Volume-5 Issue-1,March 2023

[8] A. K. Jain, *Fundamentals of Digital Images Processing*. Englewood Cliffs, NJ: Prentice-Hall, 1989.
[9] J. Short, J. Kittler, and K. Messer, "A comparison of photometric normalization algorithms for face verification," presented at the IEEE Int. Conf. Automatic Face and Gesture Recognition, 2004.
[10] C. R. González and E. Woods, *Digital Image Processing*. Englewood Cliffs, NJ: Prentice Hall, 1992.
[11] R. H. Sherrier and G. A. Johnson, "Regionally adaptive histogram equalization of the chest," *IEEE Trans. Med. Imag.*, vol. MI-6, pp. 1–7, 1987.
[12] A. Majumder and S. Irani, "Perception-based contrast enhancement of images," *ACM Trans. Appl. Percpt.*, vol. 4, no. 3, 2007, Article 17.
[13] Z. Liu, C. Zhang, and Z. Zhang, "Learning-based perceptual image quality improvement for video conferencing," presented at the IEEE Int. Conf. Multimedia and Expo (ICME), Beijing, China, Jul. 2007.
[14] E. H. Weber, "De pulsu, resorptione, audita et tactu," in *Annotationes anatomicae et physiologicae*. Leipzig, Germany: Koehler, 1834.
[15] J. Serra and P. Salembier, "Connected operators and pyramids," presented at the SPIE. Image Algebra and Mathematical Morphology

Srikanth Veesam received the Master of Technology degree in Embedded Systems from the Princeton College of Engineering and Technology-JNTUH; he received the Bachelor of Engineering degree from Princeton College of Engineering and Technology-JNTUH. He is currently working as Assistant Professor of ECE with Princeton Institute of Engineering and Technology For Women -JNTUH. His interest subjects are Embedded Systems, Microprocessors, Communication Systems, Digital Electronics and etc, Email: veesamsrikanth@gmail.com.

N. SalmaSulthana received the Master of Technology degree in VLSI System Design from the Princeton Institute of Engineering and Technology For Women-JNTUH; he received the Bachelor of Engineering degree from Dr.VRK Women's College of Engineering and Technology - JNTUH. He is currently working as Assistant Professor of ECE with Princeton Institute of Engineering and Technology For Women -JNTUH. His interest subjects are Embedded Systems, Microprocessors, Communication Systems, Digital Electronics and etc, Email: salmasulthana4u@gmail.com.